

AJP

ISSN : 0971-3093

Vol 9, No 3, July-September, 2000

ASIAN JOURNAL OF PHYSICS

An International Quarterly Research Journal



ap

ANITA PUBLICATIONS

KC-68/1, OLD KAVI NAGAR, GHAZIABAD-201 002 (INDIA)

Phones : (0575) 780506, 752552

Delhi Office : FF-47, MANGAL BAZAR, LAXMI NAGAR, DELHI-110 092 (INDIA)

Phones : (011) 2443335/36/37, 2463335/36/37, Fax : 011-2413388

The Maximum in Glass Transition Temperature (T_g) near $x = 1/3$ in $\text{Ge}_x\text{Se}_{1-x}$ Glasses

P BOOLCHAND

Department of Electrical, Computer Engineering and Computer Science,
University of Cincinnati,
Cincinnati, OH 45221-0030, USA

We review results of Raman scattering, Mössbauer spectroscopy and T-modulated Differential Scanning Calorimetry experiments on $\text{Ge}_x\text{Se}_{1-x}$ glasses. The molecular origin of the maximum in T_g near $x=1/3$ or mean coordination $\bar{r}=2(1+x)=2.67$, suggested by these experiments, implies that a *nanoscale phase separation* of the glass network takes place into Se-rich (A) and Ge-rich (B) molecular clusters. Phase separation on a molecular scale initiates at $x > 0.31$, and the B phase becomes the dominant one for $x > 0.35$. In particular, in contrast to α - and β - crystalline GeSe_2 , stoichiometric GeSe_2 glass is neither chemically ordered nor a continuous network. In ternary $\text{Ge}_x\text{As}_y\text{Se}_{1-x-y}$ glasses at $x=y$, such *nanoscale phase separation* is apparently suppressed by chemical alloying As for \bar{r} up to 3.0, and T_g s are found to *increase* continuously with \bar{r} .

1 Introduction

The physical behavior of glasses in the $\text{Ge}_x\text{Se}_{1-x}$ binary, including the extensive ($0 < x < 0.42$) bulk glass forming tendency¹ (GFT), has been a subject of profound discussions for the past three decades. These glasses display an unusually rich variety of physical phenomena ever known in the science of condensed matter, including (i) giant-photocontraction effects² in a thin-film configuration for glass compositions near a mean coordination \bar{r} of 2.40, (ii) giant-photoacoustic softening³ of the longitudinal acoustic mode for glass compositions near $\bar{r}=2.40$, (iii) existence of a thermally reversing window^{4,5} near $\bar{r}=2.40$ across which glass transitions become nearly *completely reversing* in character, (iv) optical bistability⁶ near $\bar{r}=2.67$, (v) a maximum of $T_g(\bar{r})$ ⁷ and optical band gap⁸, $E_g(\bar{r})$ near $\bar{r}=2.67$, (vi) enhanced photodiffusion and photodeposition⁹ of elemental Ag in thin-films of GeSe_2 glass, (vii) enhanced Rare-earth solubility¹⁰ in glasses for $x > 0.38$. It is widely believed that the physical effects (i-iii) taking place near glass compositions of $\bar{r}=2.40$ are related to the onset of a *floppy-to-rigid transition*¹¹ (stiffness transition) as the connectivity of the backbone increases to acquire a special value. The nature of anomalies (iv-vii) appearing near $\bar{r}=2.67$, on the other hand, are less understood. These are usually identified by the appearance of chemical order in glasses, corresponding to the existence of the stoichiometric crystalline compounds (α - and β - GeSe_2) in the

equilibrium phase diagram. A provocative suggestion¹² was made more than a decade ago that anomalies near $\bar{r}=2.67$ may arise from a dimensional regression of the *floppy to rigidity transition* from 2d-like structures prevailing at $r < 2.67$ to 3d-like structures appearing at $r > 2.67$. In this review, we re-examine the nature of physical effects taking place near 2.67. Based on spectroscopic and calorimetric results now available on the present binary and the related $Ge_xAs_xSe_{1-2x}$ ternary, it appears that the microscopic origin of anomalies near $\bar{r} = 2.67$ in the Ge_xSe_{1-x} binary can be traced to an intrinsic *nanoscale phase separation* of the glass network into Se-rich (A) and Ge-rich (B) molecular clusters. In the ternary glass system, $Ge_xAs_xSe_{1-2x}$, such phase separation is suppressed by chemical alloying As, and T_g s continue to increase monotonically with \bar{r} up to $\bar{r}=3$, thus providing a counter example. Nanoscale phase separation is difficult to detect even in diffraction experiments in crystals. In glasses the challenge is formidable, particularly if the minority phase is at the limit of detection by diffraction methods. Nevertheless, optical and thermal methods can be invaluable if the signature of such a phase separation can be established, as we presently show in this review.

2 Experimental

2.1 T-modulated differential scanning calorimetry (MDSC) results on Ge_xSe_{1-x} and $Ge_xAs_xSe_{1-2x}$

Figures 1 and 2 provide $T_g(x)$ variation in the present Ge_xSe_{1-x} binary and the $Ge_xAs_xSe_{1-2x}$ ternary. These results were obtained using T-modulated DSC (model 2920 from TA Instruments, Inc.), a recent and more sensitive variant¹³ of conventional DSC. The principal advantage of MDSC is that it permits deconvolution of the total heat flow (H_t) into a reversing (H_r) and a non-reversing (H_{nr}) component. This is achieved by programming a sinusoidal T variation over a linear T-ramp with scan rates and modulation rates that can be chosen by software commands. The reversing heat flow, H_r , is the component of heat flow that tracks the T-modulations, and displays a characteristic step-like jump from which a true measure of ΔC_p and T_g can be obtained. The non-reversing heat flow, H_{nr} , captures the kinetic effects associated with changes in network configurations as a precursor to softening of a glass at T_g .

In Fig. 1, we compare $T_g(x)$ variation in Ge_xSe_{1-x} glasses with the one in Si_xSe_{1-x} glasses, both obtained at a scan rate of 3°C/min and a modulation rate of 1°C/100 sec. Since both cations (Ge and Si) are 4-fold coordinated at low x ($x < 1/3$), the connectivity as measured by the mean coordination number $\bar{r}=2(1+x)$ is the same for the two binary networks. In both binary glass systems, $T_g(x)$ are found to generally increase with x as the glass network becomes more connected. However, a close inspection of the $T_g(x)$ trends reveals subtle differences. T_g s of the Ge-bearing glasses are somewhat *higher* than those of Si-bearing glasses at $x < 0.31$. The reverse is the case at $x > 0.31$. Particularly noteworthy is the fact that, while T_g s of Si-Se glasses *continue to increase* at $x > 1/3$, the T_g of Ge-Se glasses actually start to *decrease* at $x > 0.34$ to display a *local maximum* near $x=0.34$. The structure consequences of the threshold behavior in

$T_g(x)$ for Ge-Se glasses near $x=1/3$ is a result in want of a clear explanation, an issue we address in section 3.

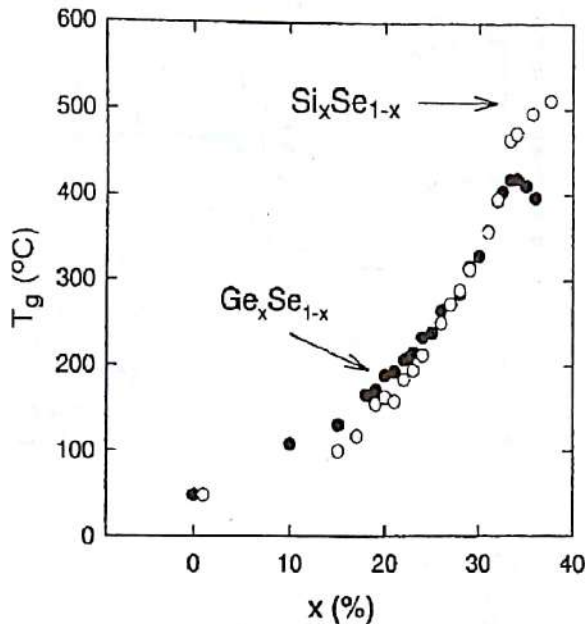


Fig. 1 $T_g(x)$ in Si_xSe_{1-x} and Ge_xSe_{1-x} bulk glasses deduced from the reversing heat flow using T-modulated DSC with a scan rate of $3^\circ\text{C}/\text{min}$ and a modulation rate of $1^\circ\text{C}/100$ sec.

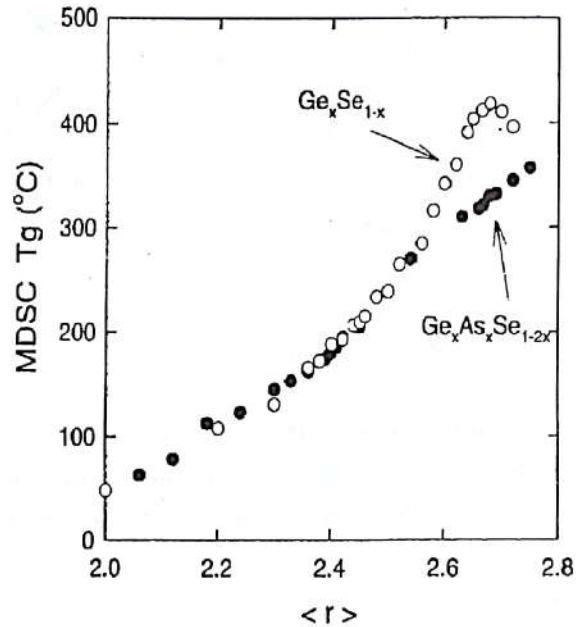


Fig. 2 $T_g(x)$ in the indicated binary and ternary bulk glasses deduced from MDSC plotted as a function of mean coordination \bar{r} , showing the threshold behavior in T_g near $\bar{r} = 2.67$ in the binary, completely suppressed upon As alloying as in the ternary.

Figure 2 displays T_g s in the $Ge_xAs_xSe_{1-2x}$ ternary. Noteworthy in these trends is the fact that T_g continues to increase with x even at $x > 0.22$. If the valences of Se, As and Ge are taken to be 2, 3 and 4, the mean coordination, \bar{r} , is given as

$$\bar{r} = 4x + 3x + (1-2x)2 = 3x + 2 \quad (1)$$

A ternary glass at $x = x_c = 2/9$ or 0.22, thus corresponds to a mean coordination of $\bar{r} = 2.67$. Chemical alloying As in a Ge-Se glass leads to a *suppression* of the threshold behavior in T_g near $\bar{r} = 2.67$. We shall return to discuss these results in section 3.

2.2 Raman scattering in Ge_xSe_{1-x} glasses

Figure 3 gives Raman scattering results on bulk Ge_xSe_{1-x} glasses (doped with a small amount of Sn) obtained near the composition $x=1/3$. Raman scattering was excited using the

647.1nm line from a Kr-ion laser and the back-scattered radiation analyzed with a triple monochromator system (model T64000 from Instruments S.A., Inc.) with a microscope attachment. The observed lineshapes display several modes, whose identification has been discussed earlier¹⁴. The modes at 200 cm^{-1} , 217 cm^{-1} , 262 cm^{-1} are associated with corner-sharing (CS) and edge-sharing (ES) $Ge(Se_{1/2})_4$ tetrahedral units and Se_n -chains, respectively. Of special interest is the mode at 178 cm^{-1} (A_1^{FS}) identified¹⁵ with ethane-like $Ge_2(Se_{1/2})_6$ units representing the signature of Ge-Ge bonds in the glasses. The scattering strength of this mode (A_1^{FS}) normalized to that of the CS-mode (A_1^{CS}) is found to increase monotonically with Ge concentration x starting at 0.31. A perusal of these results shows that for the stoichiometric glass at $x=1/3$, $A_1^{FS}/A_1^{CS} = 0.14$. The appearance of the A_1^{FS} mode at $x=1/3$ unambiguously shows that the chemical order in $GeSe_2$ glass is *intrinsically broken*¹⁶.

2.3 Mössbauer spectroscopy

Figure 4 shows ^{119}Sn Mössbauer spectra of $(Ge_{0.98}Sn_{0.02})_xSe_{1-x}$ glasses taken at liquid helium temperature with an emitter of ^{119m}Sn in $CaSnO_3$ using a standard constant acceleration drive system. The spectra show a growth in intensity of the B-site doublet feature once $x > 0.31$. The B-sites represent the signature of Ge-Ge bonds in the glasses^{16,17}. The observed lineshapes were analyzed in terms of two pairs of doublets, one centered (site A) near $v=1.50\text{ mm/s}$ and a second doublet (site B) centered near $v=2.5\text{ mm/s}$. The narrow resonance at $v = 1.50\text{ mm/s}$ is identified with Sn replacing Ge in a tetrahedral local environment - $Ge(Se_{1/2})_4$. The doublet feature B, on the other hand, is the signature of

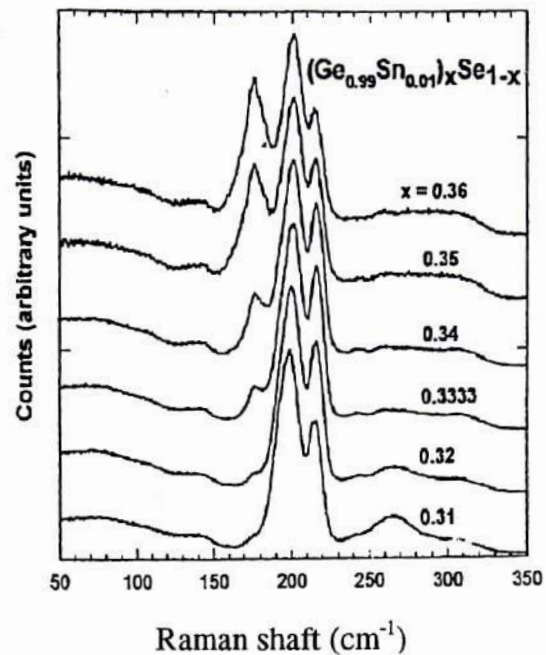


Fig. 3 Raman scattering in indicated bulk glasses showing evolution of the mode at 178 cm^{-1} with increasing Ge content.

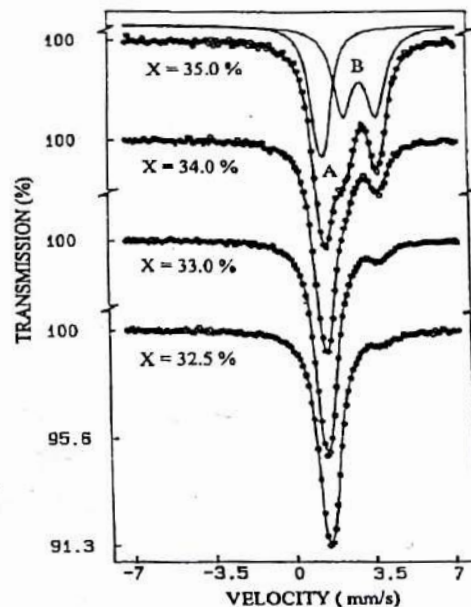


Fig. 4 ^{119}Sn Mössbauer spectra of $(Ge_{0.98}Sn_{0.02})_xSe_{1-x}$ glasses obtained at 4.2K using ^{119m}Sn in $CaSnO_3$ as an emitter. Note the growth of B-site with Ge content x .

Sn replacing Ge in an ethane-like $\text{Ge}_2(\text{Se}_{1/2})_6$ local environment. The integrated site intensity ratio, $I_B/(I_A + I_B) = I_B/I$, deduced from these Mössbauer measurements are plotted in Fig. 5(b) along with the Raman mode scattering strength ratios $A_1^{\text{FS}}/A_1^{\text{CS}}$ in Fig. 5(c), and the $T_g(x)$ variation in Fig. 5(a) in the narrow composition range $0.30 < x < 0.37$. Mössbauer experiments place $I_B/I = 0.14(1)$ in GeSe_2 glass. Both Raman scattering and Mössbauer spectroscopy *independently* reveal a systematic increase in Ge-Ge signatures in the glasses starting at $x > 0.31$. Both spectroscopies independently place the fraction of homopolar bonds in the stoichiometric glass, i.e., $N_{\text{Ge-Ge}}/N_{\text{Ge-Se}} = 1.75\%$. Four Ge-Se bonds give rise to one tetrahedral $\text{Ge}(\text{Se}_{1/2})_4$ unit, while one Ge-Ge bond gives rise to two non-tetrahedral Ge sites, thus providing approximately a factor of 8 enhancement in the broken order when measuring local sites or units in relation to counting bonds, heteropolar versus homopolar ones.

Mössbauer spectroscopy also offers the prospect to examine Se local environments in these glasses by using Te-isovalent atom substitution¹⁸. The central idea of the method is to alloy traces of 33 days $^{129\text{m}}\text{Te}$ Mössbauer parent in a Se-bearing glass of interest, and to record the emission spectrum of the glass at 4.2K in a standard ^{129}I Mössbauer spectroscopy experiment¹⁹. The oversized tracer atoms (Te) *do not randomly substitute* isovalent Se environments of a glass network, but instead preferentially replace those Se sites that have more attendant *free volume*, such as cluster-surface sites over cluster-interior ones. One of the remarkable results to emerge from these experiments on the stoichiometric GeSe_2 glass is that a *bimodal* distribution of Se-environments is tagged: an expected *chemically ordered* site (A) representing a bridging Se between two

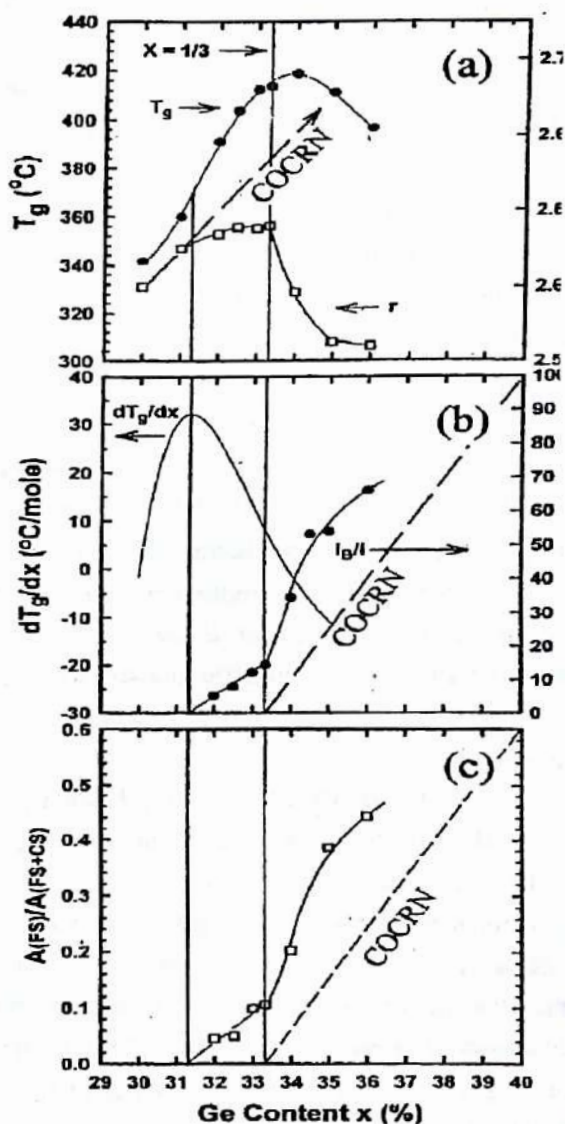


Fig. 5 (a) Compositional trends in (a) $T_g(x)$, network coordination \bar{r} (b) $dT_g(x)/dx$ and Mössbauer site intensity ratio I_B/I and (c) normalized Raman scattering strength of the 180 cm^{-1} mode as a function of x in $(\text{Ge}_{0.98}\text{Sn}_{0.02})_x\text{Se}_{1-x}$ bulk glasses. The broken-line gives the prediction of a chemically ordered continuous Random Network (COCRN) model of these glasses.

tetrahedral $Ge(Se_{1/2})_4$ units, and a *chemically disordered* site (B) associated with Ge-Se-Se signatures. The real surprise of these measurements is that Te site occupancy of B-sites exceeded that of A-sites by a factor of 20, suggesting that the Se-Se signatures (B-environments) reside on cluster surfaces while bridging Se sites (A-environments) in cluster interior. These Mössbauer spectroscopy results suggest that the oversized Te substituent in $GeSe_2$ glass apparently segregates to cluster surface sites to minimize strain by relaxing in the Van der Waals gap. Figure 6 displays ^{129}I spectra of the stoichiometric $GeSe_2$ and GeS_2 glass, as well as those of the elemental chalcogens (Te, Se and S). The close similarities in nuclear quadrupole coupling parameters (e^2qQ , η , δ) of sites A in $GeSe_2$ and GeS_2 glass on one hand, and the close parallels in quadrupole coupling parameters of site B in $GeSe_2$ -glass to those of the site observed in Se-glass, unambiguously serve to identify the proposed site assignments above^{16,17}.

The ^{129}I experiments go a step beyond the ^{119}Sn Mössbauer experiments. They not only confirm that the chemical order of $GeSe_2$ glass is *intrinsically broken*, but also show that the broken Se-chemical order must derive from the presence of *internal surfaces* native to the cluster-like (heterogeneous) morphology of the stoichiometric glass. When allowance is made for Te preference of homopolar bonds (Se-Se) in $GeSe_2$ glass, one arrives at the same degree of broken chemical order as inferred from the ^{119}Sn Mössbauer experiments, as discussed¹⁷ by us more than a decade back. These ideas are in sharp contrast to the homogeneous random network models²⁰ consisting of a network of bridging $Ge(Se_{1/2})_4$ tetrahedra as a structural description of this stoichiometric glass.

2.4 Neutron structure factor of liquid $GeSe_2$

The full power of isotopic substitution in neutron elastic scattering measurements²¹ of $GeSe_2$ liquid showed for the first time in diffraction measurements the existence of Ge-Ge and

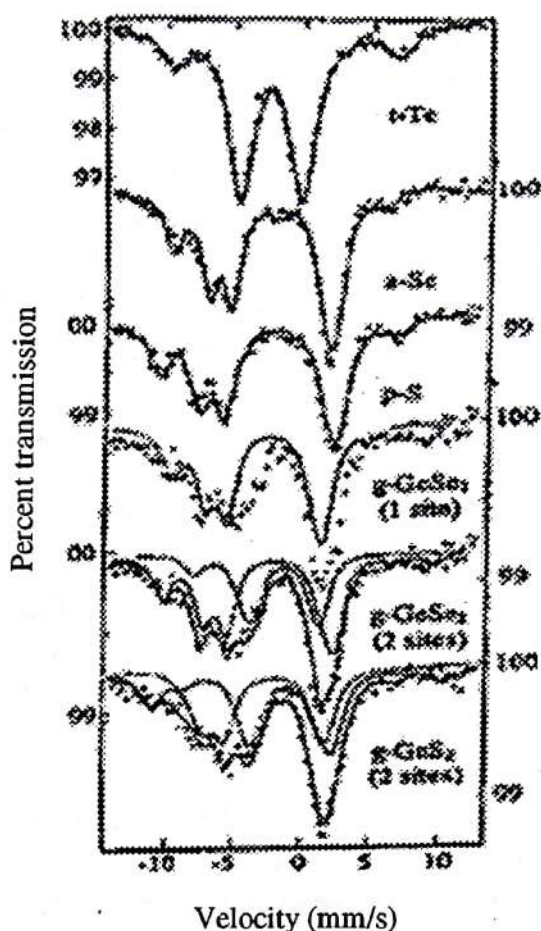


Fig. 6 Emission spectra of ^{129m}Te trace-alloyed in indicated hosts. In the elemental chalcogens, the lineshapes can be fitted to a single Te(I) environment while in the binary glasses two types of Te(I) environments are necessary to fit the observed lineshape. See text for details.

Se-Se correlations at 2.3Å, thus providing *direct evidence* for broken chemical order. It is also abundantly clear that because of the intrinsic averaging of structure information in a glassy solid and liquid, decoding aspects of gross network structure even from the highly precise partial structure factors $S_{\text{Ge-Ge}}$, $S_{\text{Ge-Se}}$, $S_{\text{Se-Se}}$ reported poses formidable challenges. Excellent fits to the measured total and partial neutron structure factors for liquid GeSe₂ of Ref. 21 have been achieved by recent first-principle molecular dynamics studies performed by Massobrio et al.²² and Drabold et al.²² Even at this level of sophistication in MD, theory is *unable to reproduce* concentration fluctuations contributing to the so called first sharp diffraction peak. These calculations also reveal that only 63% of the Ge atoms are 4-fold and 74% of the Se atoms are 2-fold, and *coexist with a sizable concentration* (30% Ge and 23% Se) of 3-fold coordinated-atoms in the liquid. These diffraction results are not consistent with Raman scattering and Mössbauer spectroscopy which place the concentration of homopolar bonds (Ge-Ge, Se-Se) in GeSe₂ glass at 1.78%, with all Ge and Se atoms thought to be 4- and 2-fold coordinated, respectively. ¹²⁹I Mössbauer spectroscopy, sensitive to the coordination²³ of the chalcogen through the sign of the nuclear quadrupole coupling, only shows evidence of 2-fold coordinated Te parent sites in the glass. Thus, in spite of the appeal of diffraction as a *direct probe* of structure, it remains uncertain at present how much information can one reliably extract on the network structure of GeSe₂ liquid and glass. Given the circumstance in GeSe₂, it is unlikely that diffraction methods possess the *sensitivity* to elucidate in a direct manner the nature of *broken chemical order* in Se-rich glasses ($x < 1/3$), as has been possible by both Raman scattering and Mössbauer spectroscopy (Fig. 5b and 5c). The small degree of broken chemical order (1.75×10^{-2}) inferred from Raman and Mössbauer spectroscopy (sections 2.2 and 2.3) is at the limit of detection for diffraction methods.

3 Glass Transition Temperature Variation and Network Connectivity

An important recent contribution to the field of glass science is due to Kerner and Micoulaut²⁴ who showed that T_g of a glass system to be an intimate reflection of network backbone connectivity. The stochastic agglomeration theory²⁵ has permitted parameterless predictions of compositional trends in T_g for binary, ternary and quaternary glass systems with rather remarkable agreement with experimental trends at low connectivities $\bar{r} < 2.40$.

3.1 $T_g(x)$ variation at low x ($x < 0.15$): stochastic regime

For the Ge_xSe_{1-x} binary glass system consisting of a 4-2 network, the slope equations²⁵ predict a linear $T_g(x)$ variation, with a maximum slope

$$dT_g(x)/dx = T_0/\ln 2 = 46\text{K}/10\text{at.}\% \text{Ge} \quad , \quad (2)$$

provided the network can be visualized as agglomerating in a random fashion upon cooling. Here T_0 is the glass transition temperature of Se glass. Taking $T_0 = 45^\circ\text{C}$ or 318K, one obtains $dT_g/dx = 46\text{K}/10$ at.% of Ge. Such a $T_g(x)$ prediction appears to be borne out by the MDSC results²⁶ on Ge_xSe_{1-x} glasses shown in Fig. 1 at low x ($x < 0.15$). At higher x , the agglomeration appears to be non-stochastic in nature as certain chemically preferred configurations appear to be selected upon structural arrest.

It is instructive to compare the $T_g(x)$ variation (Fig. 1) in Si_xSe_{1-x} glasses to the one in Ge_xSe_{1-x} glasses. At low- x ($x < 0.25$) one finds that the average slope dT_g/dx in the Si-based glasses is significantly *smaller* than the one observed in the Ge-based glasses, in spite of the fact that the single Si-Se chemical bond-strength²⁷ of 51.4 kcal/mole exceeds that of a single Ge-Se chemical bond of 49.1 kcal/mole by 4%. We thus find that simplistic ideas based on chemical bond-strength alone are inadequate to determine compositional trends in T_g . According to the stochastic agglomeration theory, the smaller slope dT_g/dx in the Si-based glass system is suggestive²⁸ of a larger degeneracy of possible bonding configurations, such as the presence of both CS and ES units in comparable amounts in the Si-based glasses, while the presence of largely CS units, in corresponding Ge-based glasses at low x . This is a point of current investigations²⁸.

3.2 $T_g(x)$ variation at medium x ($0.15 < x < 0.30$): Non-stoichiometric regime

At medium x and particularly at $x > 0.15$ corresponding to $\bar{r} = 2.30$, there is spectroscopic evidence¹⁹ to suggest that the network morphology becomes increasingly heterogeneous as rigid-fragments composed of ES and CS units are nucleated. The latter fragments qualitatively alter Te-occupancy of available Se-sites of the network as observed in ^{129}I Mössbauer spectroscopy¹⁹. One expects the *stochastic* agglomeration theory to clearly fail at this point, as indeed revealed by the super-linear variation of $T_g(x)$ once $x > 0.15$. In principle, agglomeration theory can be extended to describe non-stochastic network morphologies, but this represents a more formidable calculation in which the chemical aspects of bonding configurations need to be folded in from spectroscopic probes such as Raman scattering, Mössbauer and solid state NMR which can establish the concentration ratios of ES to CS units.

3.3 $T_g(x)$ variation at high x ($x > 0.31$): Nanoscale phase separation regime

Perhaps one of the more remarkable features of the $T_g(x)$ trends plotted in Fig. 1 is the sharply contrasting behavior of a continued *increase* at $x > 1/3$ in the Si-Se binary but a sharp turnover followed by a steady *decrease* at $x > 1/3$ in the Ge-Se binary. These contrasting behaviors in T_g , at the outset, are incompatible with simplistic ideas on chemical bond strengths as the sole factor determining T_g .

In both cases, weaker homopolar bonds²⁷ by nearly 20% (Si-Se (42.2 kcal/mole), Ge-Ge (37.6 kcal/mole)) are populated at the expense of heteropolar ones (Si-Si (51.4 kcal/mole), Ge-Se (49.1 kcal/mole)) in the glass network, yet the $T_g(x)$ trends are just opposite to each other for

these two glass systems. The central issue remains, how are these bonds incorporated in the glass network? Do they form part of the 4-2 backbone (A-phase) or do they segregate into a separate nanophase which is then attached to the A-phase? In the former case one expects the connectivity of the backbone to continue to increase with x at $x > 1/3$. This is the circumstance prevailing in Si-Se glasses where compositional trends in Raman modes show Si-Si bonds to serve as cross-links²⁹ between chain fragments of edge-sharing $\text{Si}(\text{Se}_{1/2})_4$ tetrahedra. It is for this reason that viscosities of such melts increase precipitously at $x > 1/3$ and hinder homogenization of glassy melts in Si-rich compositions unless melts are reacted for sufficient time at elevated temperature. In the latter case (Ge-Se) we suggest that the connectivity of the backbone and the viscosity of glassy melts actually decreases with x at $x > 1/3$. It is in this context that the spectroscopic and thermal results presented in Fig. 5 make a persuasive case. Both the Raman scattering and Mössbauer spectroscopy results show that nucleation of the ethane-like B-nanophase initiates near $x = 0.31$, precisely at the composition where the slope dT_g/dx actually shows a maximum. Nucleation of Ge-Ge signatures (B-nanophase) chemically decoupled from the 4-2 backbone (A-nanophase) in Ge-Se glassy melts *lower the global connectivity* of the network and therefore the slope dT_g/dx at $x > 0.31$.

Constraint counting algorithms suggest²⁶ that if the geometry of ethane-like units consists of zigzag chains rather than linear chains, a likely circumstance in a glass, the mean coordination, \bar{r}_B , of the B-nanophase is 2.56, somewhat less than the maximum \bar{r}_A of 2.64 for the A-nanophase. One can project the expected connectivity \bar{r} of the glass network, given the nanoscale phase separation model²⁶, and as expected \bar{r} shows a maximum near $x = 1/3$ (Fig. 5a), a trend that is qualitatively reflected in the observed $T_g(x)$ variation.

MDSC and Raman scattering experiments have also shown³⁰ that the nanoscale phase separation present in the Ge-Se binary can be suppressed by alloying As, as illustrated in Fig. 2. In this figure we compare $T_g(\bar{r})$ variation in the Ge-Se binary with the Ge-As-Se ternary. The threshold behavior in $T_g(\bar{r})$ observed in the binary, is now absent in the ternary. Furthermore, ¹¹⁹Sn Mössbauer spectroscopy in ternary glasses shows the absence of the B-doublet feature characteristic of the B-nanophase³⁰. These results broadly suggest that T_g of a glass network is a good representation of the global connectivity of its backbone.

4 Some Global Consequences of Nanoscale Phase Separation near $x = 1/3$ in $\text{Ge}_x\text{Se}_{1-x}$ Glasses

4.1 Glass forming tendency in $\text{Ge}_x\text{Se}_{1-x}$ and $\text{Ge}_x\text{S}_{1-x}$ glasses

Bulk glasses can be synthesized in the titled binary glass systems¹ over a wide concentration range $0 < x < 0.42$. The B-nanoscale phase plays an important role in determining the GFT in the $1/3 < x < 2/5$ concentration range because it is marginally rigid ($\bar{r} = 2.56$) and also because it is phase separated from the A-phase (4-2 network). These considerations keep

the global connectivity of Ge-rich glassy networks reasonably low ($\bar{r} \sim 2.6$) and thus promote glass formation¹¹ based on constraint counting algorithms. At higher x , a third nanoscale phase (C) composed of a distorted rock salt phase appears in these glasses³¹. The C-phase is thought to be overcoordinated ($\bar{r} = 3$) and therefore rigid and not conducive to glass formation. Bulk glass formation is thought to cease³¹ once the C-nanophase percolates when the Ge concentration x exceeds about 0.42. Thus, the intrinsic phase separation of these glasses into A-, B-, and C-nanophases, along with ideas on constraint counting algorithms, provide a good basis to understand the molecular origin of glass formation in these chalcogenides.

4.2 Nature of anomalies in physical behavior of glasses near $\bar{r} = 2.67$

Several years ago, K. Tanaka suggested¹² that the microscopic origin of anomalies in physical behavior of glasses near $\bar{r} = 2.67$ may represent a floppy to rigid transition of 2d-like structures prevailing at $\bar{r} < 2.67$ to acquire a 3d-like morphology at $\bar{r} > 2.67$. For reasons discussed earlier, the Ge_xSe_{1-x} and Ge_xS_{1-x} binaries would appear to be inappropriate glass systems to look for such a transition because of the intrinsic phase separation effects present in these glasses. There are, however, other glass systems where such phase separation effects are absent, and such systems would appear to be ideal systems to look for the transition envisaged by Tanaka, if indeed such a transition exists.

Although the $T_g(x)$ variation in the $As_xGe_xSe_{1-2x}$ ternary has been reported upon previously³² by DSC, the use of MDSC has permitted a measurement of the non-reversing heat-flow variation $\Delta H_{nr}(x)$ in this ternary³⁰ (Fig. 7) for the first time. $\Delta H_{nr}(x)$ shows a global minimum in the $0.10 < x < 0.15$ concentration range, with an order of magnitude increase both in the floppy ($x < 0.10$) and the rigid region ($x > 0.15$). The vanishing $\Delta H_{nr} \rightarrow 0$ in the $0.10 < x < 0.15$ compositional range constitutes direct evidence for the existence of a thermally reversing window, identified recently³³ with the existence of the intermediate phase surrounding the Phillips-Thorpe¹¹ transition near $\bar{r} = 2.40$.

The $\Delta H_{nr}(x)$ trend of Fig. 7 provides no evidence of an anomaly near $x = 0.22$ corresponding to $\bar{r} = 2.67$ that could be identified with a 2d – 3d stiffness transition. It is more likely that the microscopic origin of numerous anomalies¹² reported in Ge-Se based glasses near $x = 1/3$, are the consequence of an intrinsic molecular phase separation of the system.

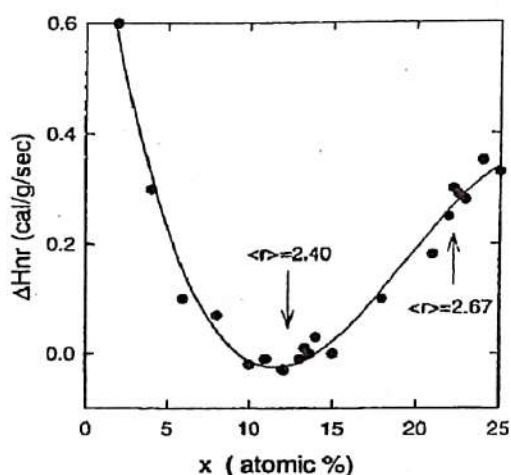


Fig. 7 Non reversing heat-flow, $\Delta H_{nr}(x)$, in the $Ge_xAs_xSe_{1-2x}$ ternary glass, showing a global minimum in the $0.10 < x < 0.15$ concentration range. No obvious anomaly is observed near $x = 0.22$ corresponding to $\bar{r} = 2.67$.

4.3 Boson peak in $\text{Ge}_x\text{Se}_{1-x}$ glasses

The microscopic origin of the Boson peak in glasses continues to be a subject of current discussions³⁴. Some of the discussion has focussed on the role of dopants in enhancing the scattering strength of the Boson peak in network glasses, while in other cases the emphasis has been on the functional form of the lineshape used to analyze the observed peak³⁵ and the interpretation of the peak frequency in the base glass. It appears that a common feature of most discussions in this regard is that the excitation is intrinsically related to the heterogeneity of glass structure. In a recent publication, Boukenter and Duvall³⁶ have reported on the Boson peak in bulk $\text{Ge}_x\text{Se}_{1-x}$ glasses, and noted the existence of a *local maximum* in scattering strength of this mode near $x = 0.34$. A natural interpretation of the Boson peak intensity maximum in $\text{Ge}_x\text{Se}_{1-x}$ glasses near $x = 0.34$ would appear to be the intrinsic nanoscale phase separation that we have eluded to in this work. It would be of interest to compare and contrast Boson peak scattering results on the Ge-Se binary with those on the Ge-As-Se ternary.

5 Concluding Remarks

The following conclusions can be drawn from the present work. (i) Raman scattering and Mössbauer spectroscopy (¹¹⁹Sn and ¹²⁹I) measurements on $\text{Ge}_x\text{Se}_{1-x}$ glass show that the chemical order of the stoichiometric glass at $x = 1/3$ is intrinsically broken. Both spectroscopic probes place the concentration of heteropolar bonds in GeSe_2 glass at slightly under 2%. (ii) Ge-Ge bonds constitute a marginally rigid ethane-like nanophase that appears not to be part of the backbone of the glass network consisting of CS- and ES- $\text{Ge}(\text{Se}_{1/2})_4$ tetrahedra. This is supported by the $T_g(x)$ trends which show a peaking out of the slope, dT_g/dx , at $x = 0.31$, at precisely the same composition where the marginally rigid ethane-like nanophase is first nucleated in $\text{Ge}_x\text{Se}_{1-x}$ glasses and, furthermore, a sharp turnover of T_g and subsequent decrease at $x \geq 0.35$ when the ethane-like nanophase becomes the majority phase. The striking correlation between the thermal (T_g) and molecular structure (spectroscopic) results is not a coincidence, but reflects changes in the network connectivity which apparently controls the T_g -variation through glass structure. In particular, the local maximum in T_g near $x = 0.34$ in the $\text{Ge}_x\text{Se}_{1-x}$ binary constitutes indirect evidence of nanoscale phase separation. (iii) In $\text{Si}_x\text{Se}_{1-x}$ glass, no evidence of broken chemical order is observed at $x \leq 1/3$ or $\bar{r} < 2.67$. Si-Si signatures first appear at $x \geq 1/3$ and form part of the backbone of CS and ES $\text{Si}(\text{Se}_{1/2})_4$ tetrahedra with T_g s continuing to increase with increasing \bar{r} , to display no threshold behavior near $\bar{r} = 2.67$. (iv) In the $\text{Ge}_x\text{As}_x\text{Se}_{1-2x}$ ternary, no spectroscopic evidence of cationic homopolar bonds is observed up to $\bar{r} \sim 3.0$, and T_g s continue to increase with \bar{r} monotonically to display no threshold behavior at $\bar{r} = 2.67$. Chemical alloying As in the Ge-Se binary, apparently suppresses nanoscale phase separation even when $\bar{r} > 2.67$.

Acknowledgements

Y. Wang, D. Selvanathan, X. Feng and W.J. Bresser participated in some of the experiments described in this review. It is also a pleasure to acknowledge discussions with M. Micoulaut, R. Kerner, E. Duval and J.C. Phillips during the course of this work. This work was supported by NSF grant DMR 97-01286.

References

1. Phillips J C, *Phys Today*, 35 (1982) 27; Also see Azoulay R, Thibierge H & Brenac A, *J Non Cryst Solids*, 18 (1975) 35.
2. Chopra K L, Harshvardhan K S, Rajgopalan S & Malhotra L K, *Solid State Commun*, 40 (1981) 387.
3. Xia H, Gump J, Finker I, Sooryakumar R, Bresser W J & Boolch P, unpublished.
4. Feng X, Bresser W J & Boolchand P, *Phys Rev Lett*, 78 (1997) 4422.
5. Boolchand P, in *Rigidity Theory and Applications*, eds Thorpe M F & Duxbury P H, (Kluwer Academic/Plenum Publishers, New York), 1999, p 279.
6. Hajto J, Janossy I & Choi W K, *J Non Cryst Solids*, 114 (1989) 304.
7. DeNeufville J P, Sarrach D & Haworth W, *J Non Cryst Solids*.
8. Street R A, Nemanich R J & Connell G A N, *Phys Rev*, B 18 (1978) 6915.
9. Kawaguchi T, Maruno S, & Elliott S R, *J Appl Phys*, 79 (1996) 9096.
10. Krasteva V, Hensley D & Sigel G, Jr *J Non Cryst Solids*, 222 (1997) 235.
11. Phillips J C, *J Non Cryst Solids*, 34 (1979) 153; Thorpe M F, *J Non Cryst Solids*, 57 (1983) 355.
12. Tanaka Ke, *Phys Rev*, B 39 (1989) 1270.
13. Wunderlich B, Jin Y & Boller A, *Thermochim Acta*, 238 (1994) 277.
14. Sugai S, *Phys Rev*, B 35 (1987) 1345.
15. Feltz A, Zickmuller K & Pfaff G, *Proc 7th Intl Conf on Amorphous & Liquid Semiconductors*, eds Spear W E & Stevenson G C, (Inst of Physics, Bristol), 1978, p 125. Lucovsky G, Nemanich R & Galeaner F, *ibid* p 130.
16. Boolchand P, Grothaus J & Suranyi P, *Phys Rev*, B 25 (1982) 2975.
17. Boolchand P, in *Physical Properties of Amorphous Materials*, eds Adler D, Schwartz B B, Steel M C (Plenum Press, New York), 1985, p 221.
18. Bresser W J, Boolchand P, Suranyi P & deNeufville J P, *Phys Rev Lett*, 46 (1981) 1689.
19. Bresser W J, Boolchand P & Suranyi P, *Phys Rev Lett*, 56 (1986) 2493; Also see R Müllmann, Mosel B D & Eckert H, *Phys Chem Chem Phys*, 1 (1999) 2543.
20. Moss S C & Price D L, *Physics of Disordered Materials*, ed Adler D, Fritzsche H & Ovshinsky S R, (Plenum, New York), p 77.
21. Penfold I T & Salmon P S, *Phys Rev Lett*, 67 (1991) 97; Boolchand P & Phillips J C, *Phys Rev Lett*, 68 (1992) 252.
22. Massobrio C, Pasquerello A & Car R, *Phys Rev Lett*, 80 (1998) 2342; Cobb M & Drabold D A, *Phys Rev*, B 56 (1997) 3054; Cobb M, Drabold D A & Cappelletti R L, *Phys Rev*, B 54 (1996) 12162; Vashishta P, et. al. *Phys Rev Lett*, 62 (1989) 1651.
23. Boolchand P, *Z Naturforsch*, 51a (1996) 572.
24. Kerner R & Micoulaut M, *J Non Cryst Solids*, 176 (1994) 271.

25. Micoulaut M & Naumis G, *Europhys Lett*, 47 (1999) 568.
26. Boolchand P & Bresser W J, unpublished.
27. Pauling L, *Nature of the Chemical Bond*, (Cornell University Press), 1960, p 85.
28. Micoulaut M, private communication.
29. Griffiths J E, Malyj M, Espinosa G P & Remeika J P, *Phys Rev*, B 30 (1984) 6978 21.
30. Wang Y, Micoulaut M & Boolchand P, unpublished.
31. Boolchand P, in *Insulating and Semiconducting Glasses*, ed Boolchand P, (World Scientific Press, Singapore), 2000, p 191.
32. Tatsumisago M, Halfpap B L, Green J LO, Lindsay S M & Angell C A, *Phys Rev Lett*, 64 (1990) 1549.
33. Selvanathan D, Bresser W J, Boolchand P & Goodman B, *Solid State Commun*, 111 (1999) 619.
34. Tikhomirov V K, Jha A, Perakis A, Sarantopoulou E, Naftaly M, Krastera V, Li R & Seddon A B, *J Non Cryst Solidsm*, 256 and 257 (1999) 89.
35. Nakamura M, Matsuda O & Murase K, *Phys Rev*, B 57 (1998) 10228.
36. Boukenter A & E Duval, *Phil Mag*, B 77 (1998) 557.

[Received : 3. 2. 2000]